XLVI CILAMCE
VITÓRIA - ES - BRAZIL - 2025
XLVI IBERO-LATIN AMERICAN CONGRESS ON COMPUTATIONAL METHODS IN ENGENEERING

Numerical modeling of tall structural masonry buildings: evaluation of wall-beam interaction in transition zones

Luiz R. S. Linhares[1], Lucas C. Pereira[1], Luciano R. Coelho[1]

[1]*Cetec Engenharia Estrutural*
Albertino de C Prestes, 18147-009, São Paulo/Araçariguama, Brazil
luiz@ceteceng.com.br, lucas@ceteceng.com.br, luciano@ceteceng.com.br

Abstract. The classification of a building as tall is not solely related to the number of stories, but also to the influence of wind loads on structural stability. As the height of buildings using this construction system increases, the challenge of implementing solutions that satisfy the Ultimate Limit State (ULS) and the Serviceability Limit State (SLS) involves, among other factors, the mathematical modeling adopted, the structural design concept, the use of concrete or masonry lintels, and the strength of the available materials. However, traditional design methodologies are often unable to account for the wide range of building typologies and may produce inconsistent results. Moreover, commercial software generally does not provide integrated modeling that considers the arching effect. In this context, numerical modeling using the Finite Element Method (FEM) stands out as a valuable tool. This study aims to evaluate the internal forces acting on transition beams in tall structural masonry buildings. Three-dimensional numerical models were developed using FEM for one tall building, with and without flange length constraints, to analyze the distribution of vertical loads as well as wind-induced forces on the transition elements. Stress concentrations were observed in both models, along with the influence of wall quantity and positioning, and the impact of model stiffness on the structural responses obtained.

Keywords: Finite Element Analysis, Arching Effect, Wall–Beam Interaction.

1 Introduction

In the current development scenario, Brazilian construction is facing challenges regarding both the quantity and qualification of the workforce. In contrast, the demand for housing continues to grow, and construction companies are increasingly seeking the adoption of structural systems with a higher degree of industrialization, with structural masonry systems in high-rise buildings standing out. These systems are characterized by material use rationalization and faster execution compared to conventional systems, as mentioned by Parsekian et al. [1] and Haseltine and Moore [2].

Structural masonry design software does not take into account the interaction between the masonry wall and the supporting structure (arch effect). One way to consider the wall-beam interaction is through three-dimensional modeling using the finite element method. Another aspect to highlight is the influence of flange length limitations in the load-bearing structure when subjected to wind actions, which can pose a challenge in designing taller buildings.

Initially, several researchers proposed simplified analytical models based on experimental results, such as in the works of Stafford Smith et al. [3], Davies and Ahmed [4], Riddington and Stafford Smith [5] and Riddington and Stafford Smith [6]. These models typically analyze the arch effect in isolated walls, where it is not possible to consider the influence of the building's overall stiffness or the effect of wind actions.

Numerical modeling has been developed to evaluate this effect, with notable studies by Lourenço [7], Barbosa [8], Medeiros [9] and Lopes et al. [10]. These works emphasize the significance of considering wall-beam interaction in structural design and its impact on the magnitude of internal forces.

Regarding flange length, the Brazilian standard ABNT NBR 16868:2020 [11] prescribes that it must be considered in the calculation of shear wall stiffness. For the interaction between masonry and supporting structure, the standard states that the load distribution must be consistent with the adopted structural scheme and that the load paths must be clearly specified. In this context, the objective of this work is to understand the load distribution in the wall-beam system in high-rise structural masonry buildings, taking into account the arch effect and the influence of flange length limitation, addressing the analysis of normal stresses and bending moments.

2 Wall-beam interaction and Limitation on flange length

The arching effect in structural masonry, addressed in the pioneering work of Wood [12], refers to the internal redistribution of forces that occurs when part of a wall transfers vertical loads to stronger lateral regions, forming a parabolic trajectory similar to an arch.

The standard ABNT NBR 16868:2020 [11] sets limitations on the length of flanges in structural masonry walls, especially when they function as "T" or "L" shaped elements in intersecting wall configurations (Fig. 1). The purpose is to prevent long and slender segments from acting without adequate lateral stability, which could compromise structural safety. The standard restricts the effective length of flanges to a maximum of six times the wall thickness, unless effective transverse tying or specific reinforcement is provided.

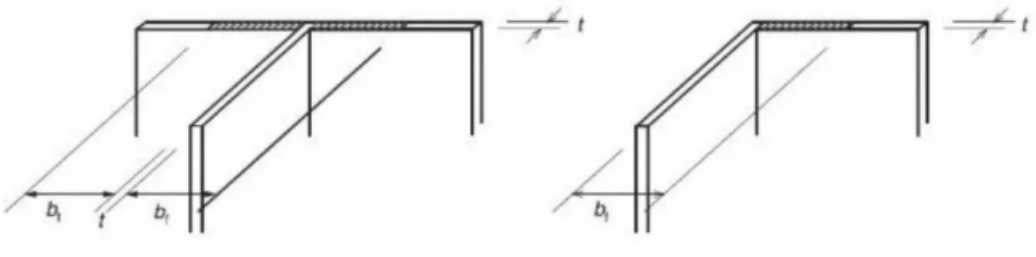


Figure 1. Effective flange length according to ABNT NBR 16868:2020 [11].

This limitation aims to ensure that the flanged segment effectively contributes to compressive or flexural-compressive strength without becoming unstable due to buckling. Exceeding this length may require additional verification through experimental testing or advanced structural modeling.

3 Methodology

To carry out the analysis, a high-rise building was selected, consisting of a ground floor, 24 floors built with structural masonry using concrete blocks with a floor-to-floor height of 2.65 meters, and a rooftop floor. The structural masonry begins above a reinforced concrete transition level composed of beams 110 cm in height and widths varying from 19 cm to 50 cm, with the typical cross-section of most beams being 25 cm by 110 cm.

As shown in Fig. 2, the building has a rectangular geometry with overall dimensions of 84.05 m by 11.14 m. On the longer facade, an expansion joint was implemented in the slab near the staircase and elevator area. For the purpose of this study, the right-side joint was selected due to greater symmetry between the walls. This joint has dimensions of 36.39 m by 11.14 m in plan and a height of 67.85 m.

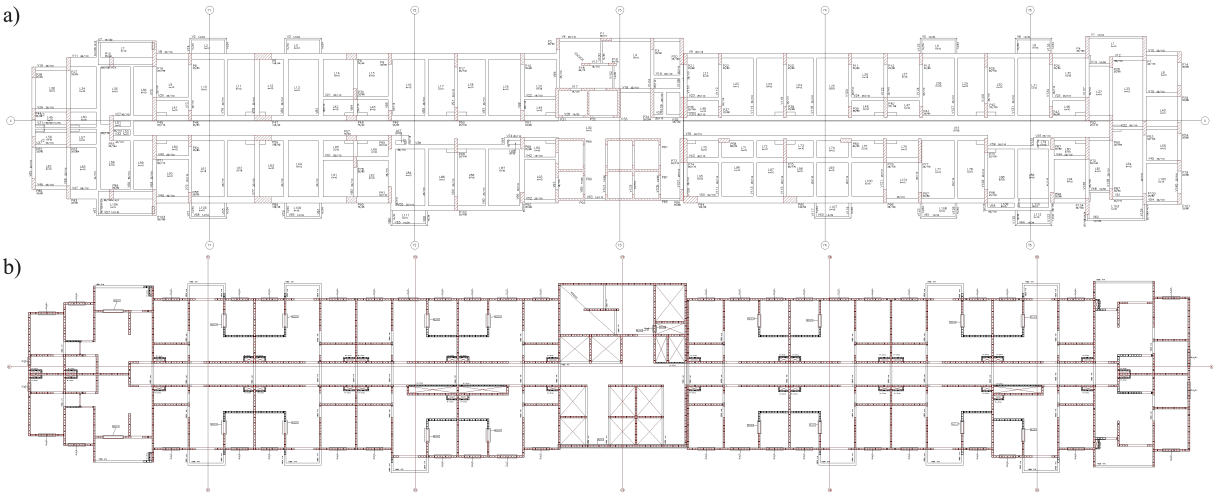


Figure 2. Building floor plans: a) layout of the 1st floor (reinforced concrete transition level); b) module layout from the 1st to the 24th typical floors.

Figure 3 shows the layout of a typical floor and the placement of concrete lintels (in blue) used to stabilize the building against wind actions in the vertical direction, in accordance with the top displacement limits established

by ABNT NBR 16868:2020 [11]. In the horizontal direction, masonry lintels were used above doors and windows on the upper and lower facades of the building. Non-structural masonry walls are marked in yellow.

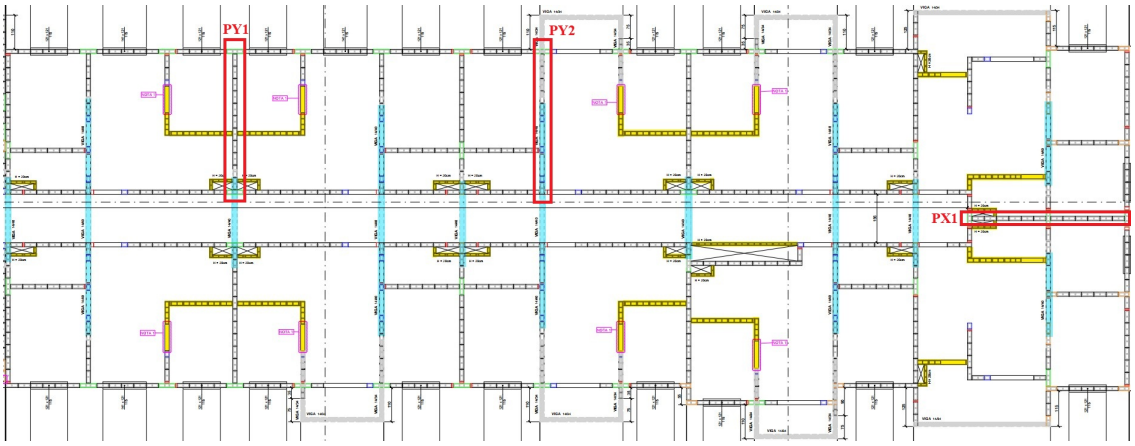


Figure 3. Labeling of the analyzed walls from the right-side joint.

For the slab loading, a permanent load of 10 kN/m² was adopted, along with the live load according to ABNT NBR 6120:2019 [13]. The loads from the 9 cm and 14 cm thick partition masonry walls were 1.40 kN/m² and 2.19 kN/m², respectively.

Regarding wind loading, according to ABNT NBR 6123:2023 [14], the following parameters were considered: basic wind speed $V_0 = 38m/s$; topographic factor $S_1 = 1.0$; land category IV; building class C; statistical factor $S_3 = 1.0$; drag coefficients (C_a) for wind acting perpendicular to the shorter and longer facades were 0.73 and 1.33, respectively.

The following conventions were adopted for directions:

- X-direction (horizontal): wind at 0° and 180° acting perpendicularly to the shorter façade, with the positive direction to the right (0°); and
- Y-direction (vertical): wind at 90° and 270° acting perpendicularly to the longer façade, with the positive direction upward (90°).

3.1 Finite Element Model Parameters

The parameters longitudinal modulus of elasticity (E_s), block compressive strength f_{bk}, and prism compressive strength (f_{pk}) are shown in Table 1.

Table 1. Properties of structural masonry.

Floor	f_{bk} (MPa)	f_{pk} (MPa)	E (MPa)	Floor	f_{bk} (MPa)	f_{pk} (MPa)	E (MPa)
Ground floor	-	-	-	11° and 12°	14	9.8	7840
1° and 2°	24	13.2	9900	13° and 14°	12	8.4	6720
3° and 4°	22	12.7	9525	15° and 16°	10	7.0	5600
5° and 6°	20	12.0	9600	17° and 18°	8	6.0	4800
7° and 8°	18	11.7	9360	19° to 21°	6	4.8	3840
9° and 10°	16	10.4	8320	22° to 24°	4	3.2	2560

To facilitate the identification of the models, the nomenclature shown in Table 2 was adopted. As observed, 12 models were developed due to the limitation in flange length and the arch effect.

For the reinforced concrete transition beams and columns, properties equivalent to a compressive strength of $f_{ck} = 40MPa$ were adopted. Regarding the material behavior, they were considered isotropic and linear elastic.For the finite element models, the software Autodesk Robot Structural Analysis Professional version 2022 was used.

Table 2. Nomenclature Adopted for the Models.

Model description	Vertical load models	Wind load models
With arch effect and with limitation 6t	M1	M1X, M1Y
With arch effect and without limitation 6t	M2	M2X, M2Y
Without arch effect and with limitation 6t	M3	M3X, M3Y
Without arch effect and without limitation 6t	M4	M4X, M4Y

The transition beams and columns were modeled with one-dimensional elements, while the slabs and structural masonry walls were modeled with two-dimensional shell elements. Figure 4 shows two of the models developed.

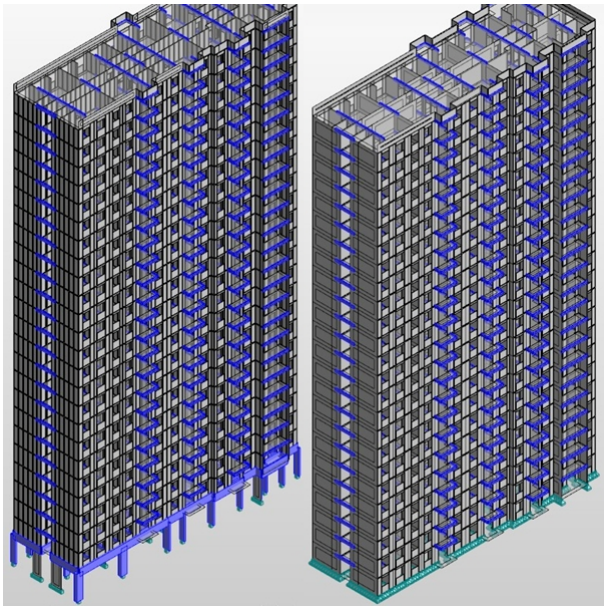


Figure 4. Finite element models M1 and M4.

A mesh sensitivity analysis was performed, and square elements with 40 cm sides were adopted. For the wind load models, a rigid diaphragm hypothesis was assumed for the slabs.

4 Results

4.1 Bending moment

For the vertical load cases, it is possible to observe in Figure 5 a reduction in the bending moment values across all analyzed walls, with the greatest difference observed for wall PY1, showing a reduction by a factor of 2.44 when the arch effect is considered. In contrast, there is an increase of 98.34% in the negative bending moment. Within the first 40 cm (half of the 6t), model M4 presents higher bending moment values, indicating wall-beam interaction near the support region. The reduction in moment for wall PY2 was by a factor of 1.58 for the positive moment, and the increase in the negative moment was 26.74%. Due to the presence of two doors, the effective wall-beam interaction length is smaller than that of PY1, which justifies the smaller difference in values, even though both have the same span and similar support conditions. Wall PX1 followed the same trend; however, the arch effect is evident at the central support, with an increase in the negative moment in the beam, as well as in the compressive stresses in the wall—an effect not observed in the model without the arch effect.

Regarding the distribution of bending moments for wind load cases, it is worth highlighting the reversal of the compressed region in wall PX1, where the consideration of the arch effect led to a condition in which the wall is entirely in tension— a situation not observed in models M3 and M4.

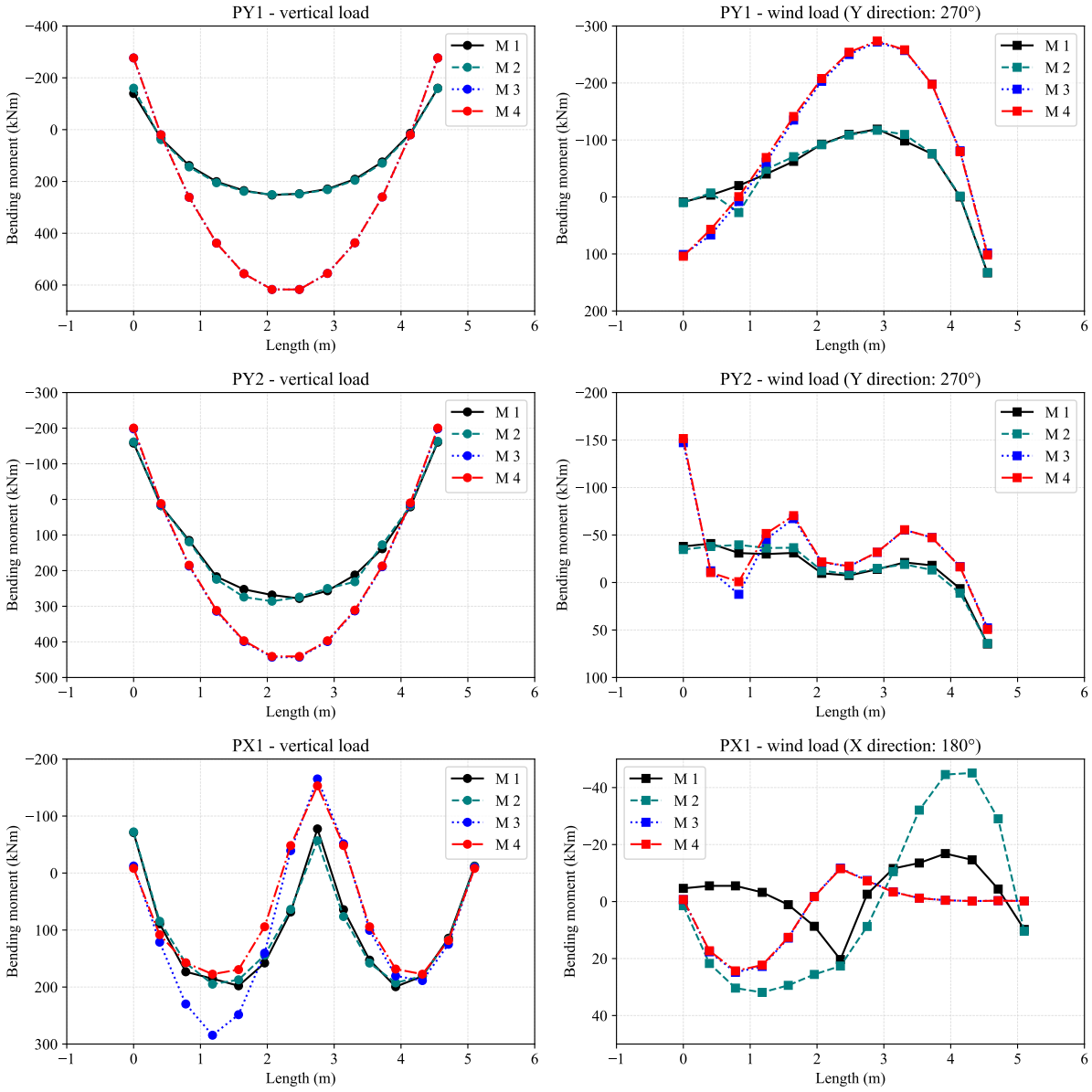


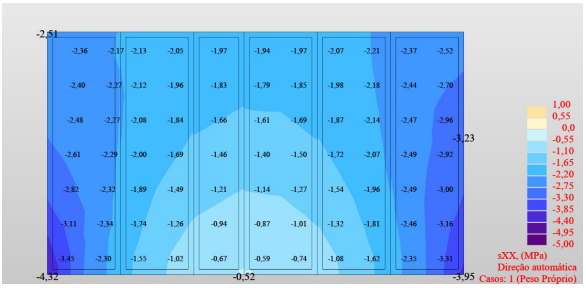
Figure 5. Bending moments in the analyzed beams.

4.2 Vertical stresses

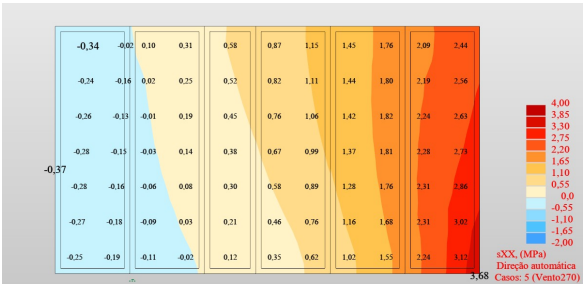
Figure 6 shows the distribution of vertical stresses in the walls for model M1, highlighting the load transfer directly to the supports, as well as the reduction in compressive stresses in the central region of the wall. Depending on the stiffness of the support beam, there is a possibility of obtaining tensile stresses that may require reinforcement in previously unreinforced regions in models that do not consider the arch effect.

By contrast, the concentration of stresses at the supports may lead to an increased need for grouting. In such cases, to approximate the service condition of the wall to the numerical model that assumes perfect bond between elements, it is necessary for both of these characteristics to be properly detailed in the structural design.

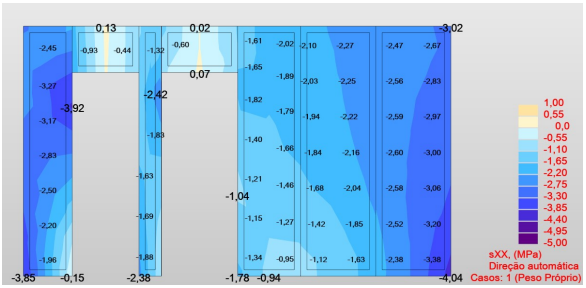
As previously mentioned, model M1X for the 270° wind load case shows tensile stresses along the entire length of the wall. This indicates that, depending on factors such as wind intensity and building geometry, stress combinations may result in reinforced segments longer than those observed in models M1 and M2.



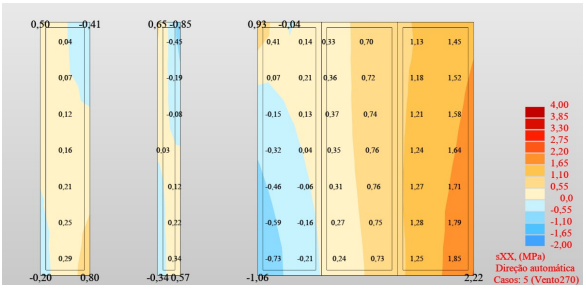
(a) PY1 - Model M1



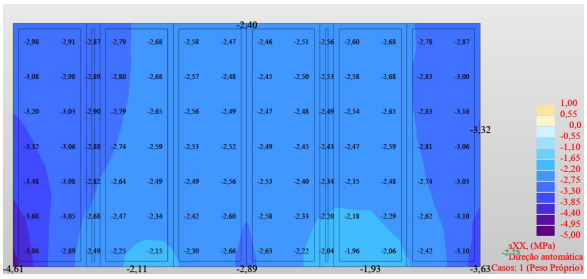
(b) PY1 - Model M1Y



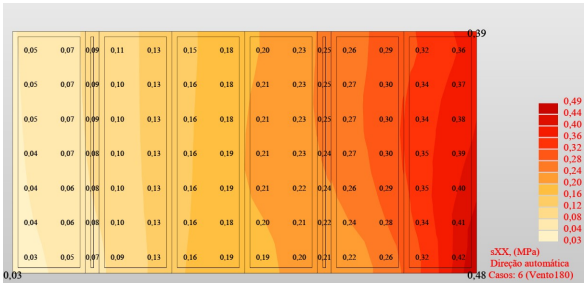
(c) PY2 - Model M1



(d) PY2 - Model M1Y



(e) PX1 - Model M1



(f) PX1 - Model M1X

Figure 6. Vertical stresses in the analyzed walls.

Table 3 presents a summary of the maximum vertical stress values obtained for all the models studied.

Table 3. Maximum vertical stresses σ_{xx} at the wall ends.

Wall	Model	σ_{xx} (MPa)	Wall	Model	σ_{xx} (MPa)	Wall	Model	σ_{xx} (MPa)
PY1	M1Y	+3.68/-3.68	PY2	M1Y	+2.22/-2.22	PX1	M1X	+0.48/-0.48
PY1	M2Y	+3.56/-3.56	PY2	M2Y	+2.05/-2.05	PX1	M2X	+1.34/-1.34
PY1	M3Y	+3.72/-3.72	PY2	M3Y	+2.13/-2.13	PX1	M3X	+0.57/-0.57
PY1	M4Y	+3.58/-3.58	PY2	M4Y	+1.89/-1.89	PX1	M4X	+1.63/-1.63

Regarding the arch effect, walls PY1 and PX1 showed stresses that were 1.07% and 18.75% higher, respectively, for models M1 and M3. In wall PY2, this behavior was the opposite, with model M3Y showing a stress 4.22% lower than model M1Y. This can be explained by the presence of openings, as previously mentioned in relation to bending moments. Despite the similarity in maximum wind stress values, when comparing the stress distribution along the length of the wall, significant differences and inversions between tensioned and compressed regions were observed between the models with and without arching effect.

The limitation in flange length showed a greater difference in wall PX1, with stress 179% higher in model M2 compared to model M1 for the case with the arch effect, and 186% higher in model M4 compared to model M3 without the arch effect.

Regarding the maximum stresses due to vertical load, model M1 presented stresses 59.41%, 33.33%, and 73.30% higher compared to model M3, for walls PY1, PY2, and PX1, respectively.

5 Conclusions

From this study, the following aspects were observed:

- the transition elements must be designed considering all internal forces, including shear force, axial force, and torsion (not addressed in this work), as well as the eccentricity between the wall and the support beam, as highlighted by Lopes et al. [10];
- the wall-beam interaction increases the concentration of stresses in the wall under vertical loads or wind action and must be designed in accordance with ABNT NBR 16868:2020 [11]; and
- although the arch effect occurs predominantly at the transition floor, full building modeling provides a more accurate assessment of horizontal force distribution in the support elements compared to analytical models, especially regarding the possibility of torsion along the height.

The percentage differences obtained in this analysis are specific to the building studied under the conditions described and cannot be generalized to all cases and support conditions. However, for the modeling of high-rise masonry buildings considering the arch effect, a similar behavior is expected in terms of load distribution in the wall-beam system.

Acknowledgements. CETEC ENGENHARIA ESTRUTURAL for their essential support in providing the tools and technical resources that enabled the completion of this work.

Authorship statement. The authors hereby confirm that they are the sole liable persons responsible for the authorship of this work, and that all material that has been herein included as part of the present paper is either the property (and authorship) of the authors, or has the permission of the owners to be included here.

References

[1] G. A. Parsekian, A. A. Hamid, and R. G. Drysdale. *Comportamento e Dimensionamento de Alvenaria Estrutural*. EdUFSCar, São Carlos, 2 edition, 2014.
[2] B. A. Haseltine and J. F. A. Moore. *Handbook to BS-5628: Structural Use of Masonry. Part 1: Unreinforced Masonry*. The Brick Development Association, London, 1981.
[3] B. Stafford Smith, M. Khan, and H. Wickens. Tests on wall-beam structures. In *Proceedings of the International Symposium on Load-Bearing Brickwork*, pp. 289–303, London. British Ceramic Society, 1977.
[4] S. Davies and A. Ahmed. An approximate method for analyzing composite walls/beams. In *Proceedings of the International Symposium on Load-Bearing Brickwork*, pp. 305–320, London. British Ceramic Society, 1977.
[5] J. Riddington and B. Stafford Smith. The composite behavior of elastic wall beam systems. *Proceedings of the Institution of Civil Engineers, Part 2*, vol. 63, pp. 377–391, 1977.
[6] J. Riddington and B. Stafford Smith. Composite method of design for heavily loaded wall-beam structures. *Proceedings of the Institution of Civil Engineers, Part 1*, vol. 64, pp. 137–151, 1978.
[7] P. Lourenço. Computational strategies for masonry structures. M.s. dissertation, Delft University of Technology, Delft, 1996.
[8] P. C. Barbosa. Estudo da interação entre paredes de alvenaria estrutural com vigas de concreto armado. M.s. dissertation, Universidade de São Paulo, Escola de Engenharia de São Carlos, São Carlos, SP, 2000.
[9] K. A. S. Medeiros. Modelagem computacional para avaliação da interação entre painéis de alvenaria e estrutura de suporte em concreto armado. M.s. dissertation, Universidade Federal do Rio Grande do Norte, Natal, RN, 2015.
[10] A. C. S. Lopes, do J. A. Nascimento Neto, de K. A. Sousa Medeiros, and D. N. Maciel. Three-dimensional modelling of wall-beam interaction in structural masonry buildings. *Revista IBRACON de Estruturas e Materiais*, vol. 13, n. 4, pp. e13414, 2020.
[11] Associação Brasileira de Normas Técnicas, NBR 16868, Alvenaria estrutural - Parte 1: Projeto, ABNT, 2020.
[12] R. Wood. Studies in composite construction. part 1: The composite action of brick panel walls supported on reinforced concrete beams. Technical Report 13, Her Majesty's Stationery Office, London, 1952.
[13] Associação Brasileira de Normas Técnicas, NBR 6120, Ações para o cálculo de estruturas de edificações, ABNT, 2019.
[14] Associação Brasileira de Normas Técnicas, NBR 6123, Forças devidas ao vento em edificações, ABNT, 2023.